Eur. Phys. J. D **20**, 389–398 (2002)
DOI: 10.1140/epjd/e2002-00146-7

THE EUROPEAN PHYSICAL JOURNAL D

Infrared ion dip and ultraviolet spectroscopy of 4-phenyl imidazole, its tautomer, 5-phenyl imidazole, and its multiply hydrated clusters

F.O. Talbot and J.P. Simons[a]

Physical and Theoretical Chemistry Laboratory, South Parks Road, Oxford OX1 3QZ, UK

Received 20 December 2001
Published online 13 September 2002 –

Abstract. Mass-resolved resonant two photon ionisation (R2PI) and infrared ion dip spectra have been recorded for 4-phenylimidazole (4PI) and its singly and multiply hydrated clusters $4PI(H_2O)_{n=0-4}$, under supersonic expansion conditions. In the case of $4PI(H_2O)_{0,1}$, it has also been possible to record infrared spectra in both the ground (S_0) and excited (S_1) states. Combining the experimental data with the results of *ab initio* calculations has led to the structural assignment of each cluster. In each case, the water molecules bind primarily to the NH site of the imidazole ring. Clusters with $n \geq 2$ incorporate linear water chains, in which the proton donating terminus bridges either to the π-electron system ($n = 2$) or to the >N: atom site ($n = 3, 4$) on the imidazole ring. Despite the creation of a "water wire", connecting the donor and acceptor sites of imidazole, there is no evidence of proton transfer in either the ground or excited state.

PACS. 36.40.Mr Spectroscopy and geometrical structure of clusters

1 Introduction

In the last few years several groups have exploited the low temperature environment of a free jet, gas phase expansion to prepare isolated and structurally assigned, solvent-bridged molecular clusters. The ready formation of water chains linking donor and acceptor hydrogen-bond sites has been established in systems such as 2-pyridone and 2-hydroxy pyridine [1–3], 7-hydroxyquinoline [4,5], 3, 4-dihydro-2(1H)-quinoline and oxindole [6], 7-azaindole [7], trans-N-phenyl formamide [8,9], 9(10H)-acridone [10] (despite the unfavourable relative orientation of the >NH and >C=O binding sites), the syn conformers of carboxylic acids (linking the OH and C=O sites) [11–13] and the amino acid, tryptophan (between the OH and >C=O or the OH and amino group sites) [14]. In some cases, these investigations have been used to explore the possibility of enol↔keto tautomer interconversion, *e.g.* in the cyclic amides, 2-pyridone [1,2] or 7-hydroxyquinoline [4,5,15,16], mediated through proton transfer along the hydrogen-bonded water, ammonia or mixed solvent molecular chains. *Ab initio* computations for (the appropriate conformers of) tryptophan. $(H_2O)_n$ suggest the possibility of proton transfer leading to zwitterion formation, for water chain lengths, $n \geq 3$.

In the amino acid, histidine, the presence of both >NH and >N: sites in the imidazole ring allows it to function both as a donor and an acceptor in a hydrogen-bonded environment. Its combined operation as an acceptor (from the hydroxyl group of a serine residue) and a donor (to the carboxylate ion in an aspartate residue) in the hydrogen-bonded triad sites is thought to play a crucial role in promoting the enzyme's catalytic activity [17,18]. In an aqueous medium, 4-methyl imidazole equilibrates to a mix of the 4- and 5-tautomers [19] and in this environment the conduits for proton transfer could be provided by transient, solvent bridged structures linking the donor and acceptor sites, so-called "proton wires" [20,21]. Proton transfer between the two nitrogen sites results in tautomeric inter-conversion[1]. The incidence and mechanism of proton transfer along water chains, both in condensed phase chemical and biological environments and in isolated clusters in the gas phase, is under sustained current (theoretical) debate [20,21], though, as Zwier has recently observed [22] the role of water "wires" "is difficult to prove (experimentally)". A logical strategy for

[a] e-mail: john.simons@chem.ox.ac.uk

[1] An earlier gas phase spectroscopic study of 4-phenyl imidazole [23] also revealed a tautomeric inter-conversion during its passage through the pulsed nozzle valve (presumably on the metal surfaces); this allowed a parallel ultraviolet spectroscopic investigation of the 5-phenyl tautomer to be completed. 2-hydroxy pyridine behaves in a similar way, converting to its keto tautomer, 2-pyridone [1].

experimentalists proposed by Leutwyler [15], includes three components: "the construction of a molecular "scaffold" with defined proton injection and extraction sites (into and out of the water chain); a triggering event (typically photon absorption); and detection of the result of proton transfer (into or through the H-bonded chain)." Two recent studies of the electronic spectra of jet-cooled 4-phenyl imidazole (4PI), its singly hydrated complex, and its tautomer, 5-phenyl imidazole (5PI), conducted at intermediate [23] and high [24] resolution, represent the first step in this sequence. 4PI is planar in its ground electronic state (S_0) but its tautomer, 5PI, is twisted about the inter-ring axis by 27°; in the S_1 state both tautomers become planar. In the hydrated complex, the water molecule binds preferentially at the >NH site, accepting a proton from the imidazole ring.

A number of questions arise from this work. Would the doubly hydrated cluster form a donor (D)–acceptor (A) assembly, D-4PI-A, to provide a model "triad" system, or would the preference be for the binding of a water dimer either as a proton acceptor or as a proton donor (as for example, in trans-N-phenyl formamide. $(H_2O)_2$ [8,9] where both NH donor and C=O acceptor complexes are formed)? Could the >N: and NH groups be bridged by an extended water chain and if so, how many water molecules would be required? Could such a chain provide a conduit for proton transfer, either in the ground or the excited state, leading to 4PI→5PI tautomer inter-conversion? In an attempt to answer at least some of these questions, the present work describes the results of an extended computational, spectroscopic, and structural study of the series of hydrated clusters, $4PI{\cdot}(H_2O)_{n=0\rightarrow4}$.

2 Computational and experimental procedures

2.1 Ab initio calculations

Calculations were performed using the Gaussian98 [25] software package, principally at the B3LYP/6-31+G* level of theory, following procedures similar those used earlier [23]. All structures were fully optimised and harmonic frequencies were calculated at each minimum. The N–H and O–H frequencies were scaled by the usual factors, 0.965 and 0.975 respectively, that have been successfully employed in earlier studies of several amide-water clusters [26–28]. All relative energies tabled include the scaled zero point corrections and are corrected for BSSE using the counter-poise method [29].

2.2 Mass-selected resonant two photon ionisation and infrared ion-dip spectroscopy

Mass-selected resonant two photon ionisation (MS-R2PI) spectra were recorded using a YAG laser-pumped, frequency-doubled dye laser (LAS) operating at wavelengths in the range 280–295 nm and bandwidths of 0.3 cm^{-1}. 4- (and 5-) phenyl imidazole (from Aldrich) was expanded in helium through a pulsed nozzle valve (0.5 mm orifice, stagnation pressure 2−4 bar, sample oven temperature 385 K) and ion signals were detected *via* a differentially pumped, time-of-flight mass spectrometer (R.M. Jordan). Hydrated clusters were formed by seeding the carrier gas with (de-ionised) water vapour. Infrared ion dip (RIDIR) spectra were recorded with the UV laser probing the $S_1 \leftarrow S_0$ transition of interest while scanning the counter-propagating IR laser. The tunable IR laser radiation (*ca.* 3 000–4 000 cm^{-1}, 1 cm^{-1} bandwidth, 1.5 mJ/pulse) was obtained by a Continuum difference frequency-mixing module at the output of a Nd:YAG-pumped Continuum ND6000 dye laser, operating with the LD765 dye. The IR beam was focused onto the jet antiparallel to the UV beam. The delay between the IR and UV lasers was set to 100 ns, to record vibrational spectra in the ground, S_0 state, and to 0 ns to record vibrational frequencies in the excited, S_1 state.

Table 1. Inter-ring angle (τ), rotational constants and inertial defect (ΔI) of 4PI. Both *ab initio* methods use the 6-31+G* basis set. Experimental values were obtained from analysis of rotationally resolved spectra [24].

	RHF+MP2	B3LYP	experimental
τ / deg	28.9	0.0	0
A / MHz	3 541.7	3 561.5	3 565
B / MHz	677.8	681.0	685.4
C / MHz	579.4	571.7	575.6
ΔI / u Å^2	−16.0	0	−1.1

3 Results

3.1 Ab initio predictions

4PI and 5PI

Although previous *ab initio* calculations of the twisted equilibrium structure in 5PI were in reasonable agreement with experiment at the HF/6-31G* and MP2/6-31G* levels, they did not predict the planar structure of its tautomer, 4PI. Inclusion of diffuse functions did not improve the situation; calculations at the MP2/6-31+G* level predicted a torsional angle of 29° for 4PI [23]. The B3LYP hybrid functional, however, with the same basis set does predict a fully planar 4PI (C_s symmetry). Table 1 shows the calculated rotational constants and inertial defects obtained with both methods. The B3LYP functional also predicts a non-planar equilibrium structure for 5PI with an angle of 27° between the rings and a torsional barrier of 121 cm^{-1}. These values are in remarkably good agreement with the experimentally determined ones of 27° and *ca.* 90 cm^{-1} [24]. The (scaled) harmonic vibrational frequencies predicted at the B3LYP/6-31+G* level will also be seen (see Sect. 4) to be in very good agreement with experiment.

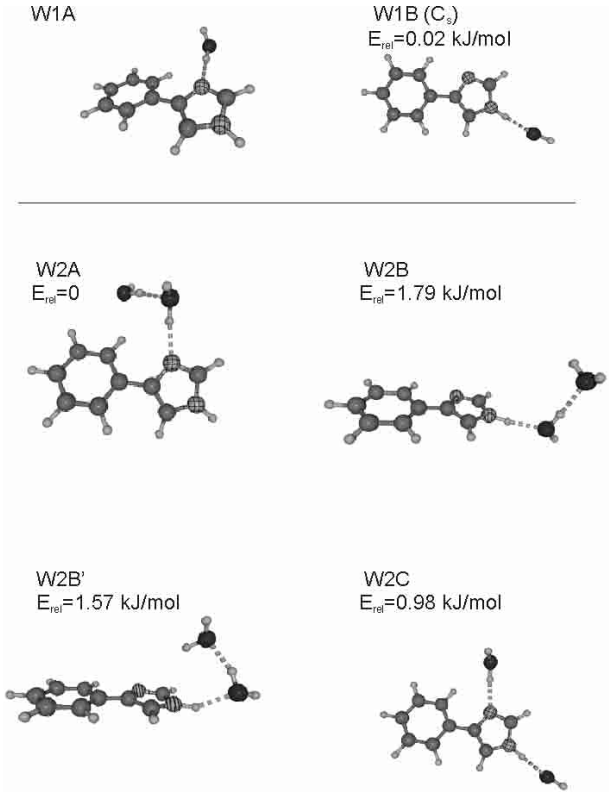

Fig. 1. Lowest energy conformers of 4PI·(H_2O) and 4PI·(H_2O)$_2$; structure and relative energies (including BSSE corrections) calculated at B3LYP/6-31+G* level of theory.

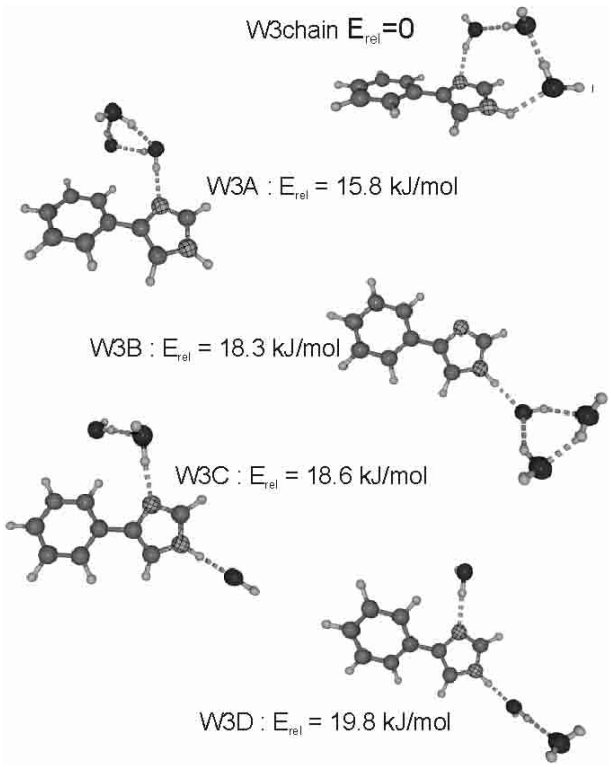

Fig. 2. Predicted *ab initio* structures of the 4PI·(H_2O)$_3$ cluster; structure and relative energies (including BSSE corrections) calculated at B3LYP/6-31+G* level of theory.

4PI(H_2O)

In the most stable, singly hydrated cluster structure W1B (see Fig. 1), 4PI acts as a proton donor, (NH→O_{water}), and the C_s symmetry is retained. The alternative structure, W1A, in which water acts as a proton donor, (OH → N), destroys the planarity of 4-PI, twisting its two rings through a torsional angle of 16.5°. The two structures are predicted to lie relatively close in energy (due no doubt to the stabilisation introduced into W1A by a weak, $O_{water} \rightarrow HC_{phenyl}$ hydrogen-bond), with W1B being the more stable, by *ca.* 0.6 kJ mol^{-1}, but slightly the less stable after including the BSSE correction.

4PI(H_2O)$_2$

The doubly hydrated cluster can adopt three distinct structures accommodating either a dimer, attached at the >N (W2A) or the >NH imidazole ring sites (W2B and W2B′), or two single water molecules bound at both sites (W2C). Although the most stable structure is predicted to be W2A, the alternatives are calculated to lie quite close in energy (see Fig. 1). Like the singly hydrated cluster, correcting for the BSSE generates some changes in the relative energies: conformer W2C suffering from less BSSE than the W2B, ends up below it, although predicted to lie ∼0.6 kJ mol^{-1} higher, before correction. The W2B structure exists in two variants: an open chain where the second water molecule is only an H-bond acceptor, and a π-bonded chain where the second water forms an OH···π H-bond with the imidazole ring (W2B′). This alternative structure proved to be very difficult to optimise with the B3LYP/6-31+G* method as the maximum step size allowed during the optimisation had to be halved to prevent the structure from going back to W2B. This π-bonded, W2B′ conformer, is predicted to be slightly more stable than the "open" W2B structure by 0.2 kJ mol^{-1}, lying just 1.57 kJ mol^{-1} above the W2A structure.

4PI(H_2O)$_3$

As with the doubly hydrated clusters, the DFT calculations predict several alternative low-lying structures, accommodating either a water ring trimer bound to the >N: site as a proton donor (W3A), or as an acceptor at the >NH site (W3B), or accommodating a water dimer, bound at the >N: or the >NH sites, together with a single water molecule bound at the >NH (W3C) or the >N: (W3D) sites, see Figure 2. A new structure is however now possible where the three water molecules form a chain of hydrogen bonds, bridging the >NH and >N sites of the imidazole ring (W3chain). Although this "daisy chain" of H-bonds is very constrained (the two hydrogen bonds binding to the imidazole being very non-linear), it benefits greatly from cooperativity effects and is by far the

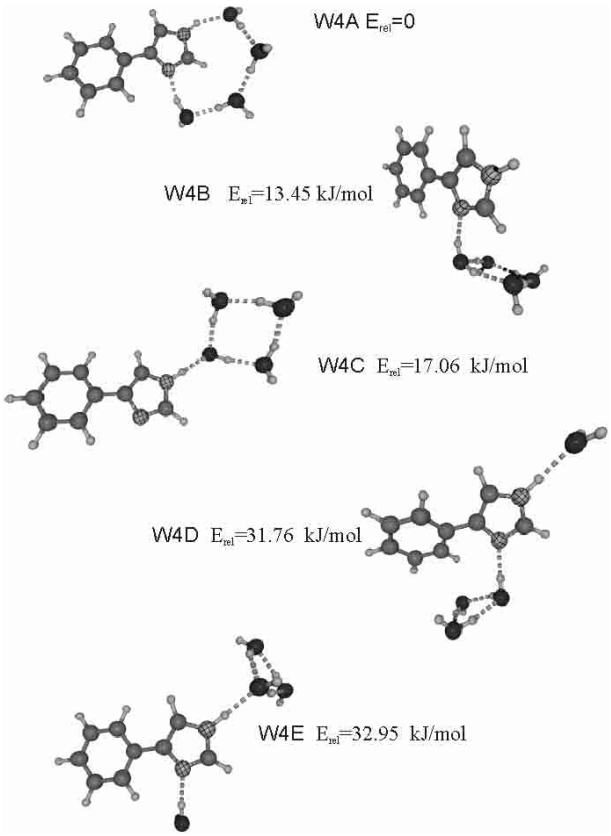

Fig. 3. Predicted *ab initio* structures for 4PI·$(H_2O)_4$; structure and relative energies (including BSSE corrections) calculated at B3LYP/6-31+G* level of theory.

most stable structure, lying ∼16 kJ mol^{-1} below the others. A further consequence of this structure is a twisting of the inter-ring dihedral angle of ∼15°. The twisting is an electronic rather than a steric effect since the water chain is located well above the imidazole ring. Each of the computed structures is predicted to display a distinctly different IR spectral signature. The second-lowest energy structure, for example, W3A, will display two bands only in the region of the "free" O–H stretching mode, while the cluster structures W3chain and W3B would display three, and the alternative structures W3C and W3D, would each display four.

4PI$(H_2O)_4$

Although the *ab initio* calculations predict five alternative structures for the 4PI$(H_2O)_4$ cluster (see Fig. 3) the global minimum structure (W4A), in which the >N: and >NH sites of the imidazole ring are linked by a chain of four water molecules, is predicted to be much the most stable. The structures accommodating a cyclic water tetramer attached to the 4PI host at either the >N: (W4B) or >NH (W4C) H-bonding sites, are considerably less favoured and the two "mixed" structures (W4D,E), incorporating a trimer and monomer attached to both sites of the imidazole ring, lie at even higher energies. The

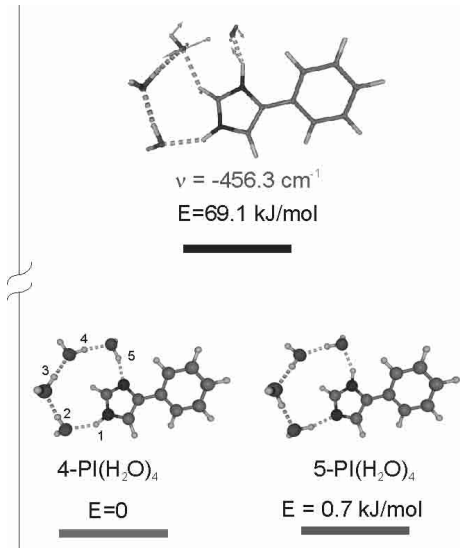

Fig. 4. Transition state for the tautomeric proton transfer from the 4PI·$(H_2O)_4$ to the 5PI·$(H_2O)_4$ cluster.

"water-wire" structures of the two tautomers, 4PI$(H_2O)_4$ and 5PI$(H_2O)_4$, which are the most likely to promote proton transfer and tautomer inter-conversion, are very similar, having inter-ring torsional angles of 18° (4PI) and 20.5° (5PI). The two clusters are also nearly iso-energetic in the ground state, with the 5PI cluster predicted to lie only 0.8 kJ mol^{-1} above its 4PI$(H_2O)_4$ equivalent (structure W4A)[2]. They are separated however by a high barrier, with a minimum energy transition state predicted to lie some 70 kJ mol^{-1} above the two minima (see Fig. 4). This transition state was found by first scanning the potential energy surface of the complex (no relaxation was allowed); it then appeared that motion of the hydrogen H5 was the least expensive energetically. A series of scans were performed along the r5 (O4–H5) coordinate with the proton H4 at various positions until the curve showed a distinct maximum followed by a minimum. The corresponding values of r4 and r5 were then used in the starting structure for the search of a fully optimised transition state. The negative frequency (−456.3 cm^{-1}) is too low for a pure H atom motion, indicating some heavy atom rearrangement. This is confirmed by the associated normal coordinate represented by arrows in Figure 4: the main motions are localised on the two protons H4 and H5, with some motion also on the O4 and O5 oxygen atoms.

3.2 Spectroscopy of 4PI and its water clusters

R2PI spectra of the hydrated clusters of 4PI, recorded in the mass channels, 4PI·$(H_2O)^+_{n=0-4}$, are shown in Figure 5. They display series of resolved vibronic bands in the region 34 600–35 100 cm^{-1} (∼200 cm^{-1} to the red of the

[2] At the B3LYP/6-31++G** level, the difference, 0.08 kJ mol^{-1} is even lower.

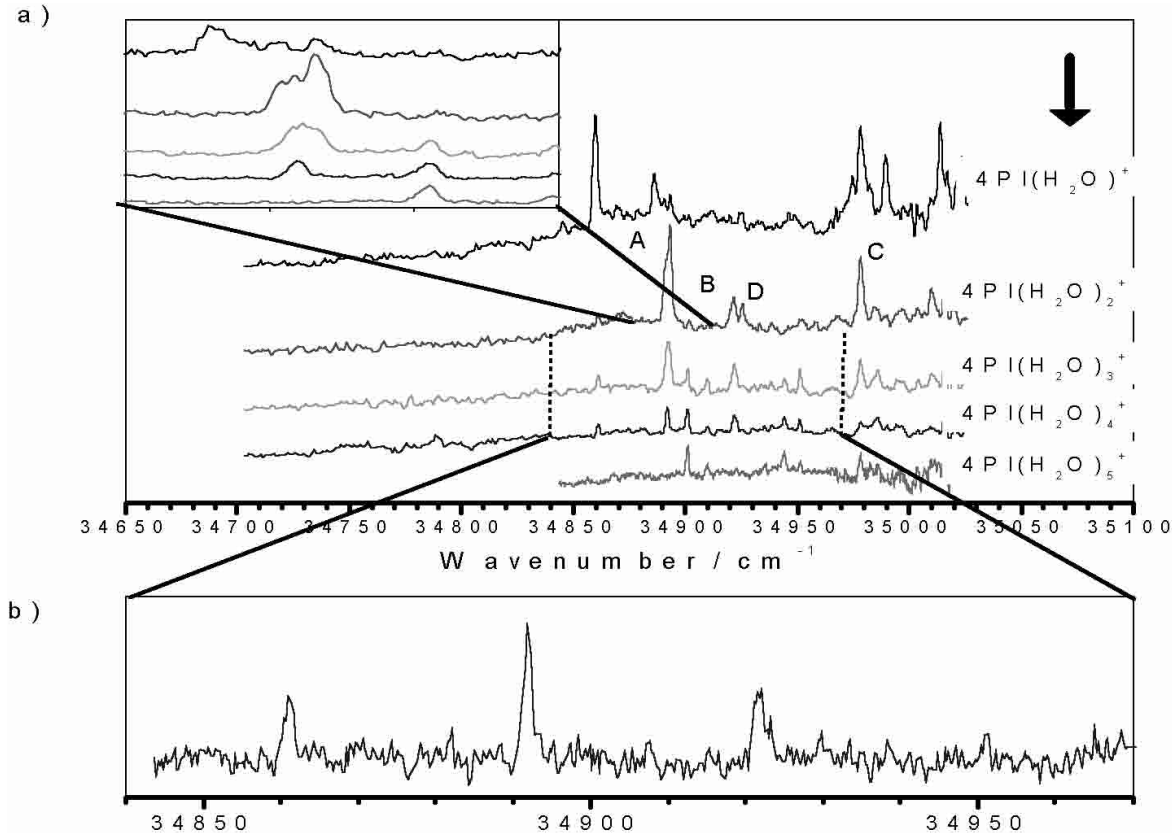

Fig. 5. (a) One-colour-R2PI spectra recorded in the 4PI·$(H_2O)_{n=1...4}$ mass channels, in the 34 600–35 100 cm^{-1} region. The arrow indicates the position of the monomer's band origin. (b) R2PI spectrum of the 4PI·$(H_2O)_4$ cluster, obtained by subtracting the spectrum recorded in the $n = 5$ channel from that in the $n = 4$ mass channel.

monomer's spectrum), associated with the $S_1 \leftarrow S_0$ transition. Many bands appear in more than one mass channel, reflecting the incidence of extensive cluster ion fragmentation. Bands associated with clusters with $n \geq 3$, for example, could be recorded in the n, $n-1$ and $n-2$ mass channels, indicating evaporation of up to two water molecules; to establish their individual assignments unambiguously, their IR ion-dip spectra were recorded in all three mass channels. Bands due to 4PI$(H_2O)_2$, 4PI$(H_2O)_3$, and 4PI$(H_2O)_4$ clusters all appear in the 4PI$(H_2O)_2^+$ mass channel and are labelled "A"..."D" in Figure 5.

4PI

The IR-UV ion dip spectra of the monomers of 4PI and 5PI display a single intense band associated with the ν(NH) stretching vibration, lying at 3 514 cm^{-1} (4PI) and 3 506 cm^{-1} (5PI) respectively, close to the liquid phase value of ∼3 500 cm^{-1} [30] (see Fig 6).

4PI(H_2O)

Only one mono-hydrated cluster could be identified in the UV "hole-burned" MS-R2PI spectrum recorded in the ion channel associated with 4PI$(H_2O)^+$. The origin band, located at 34 865 cm^{-1} and shifted 209 cm^{-1} to the red of the origin band in the 4PI monomer has already been assigned to the 4PI(H_2O) complex [23]. The trace (b) in Figure 6 shows the corresponding IR ion dip spectrum which now displays the "free", symmetric and anti-symmetric stretches of the water molecule, lying at 3 656 and 3 747 cm^{-1}, respectively. The ν(NH) stretching band at 3 409 cm^{-1}, is displaced by 104 cm^{-1} to the red of the monomer frequency. Such a shift clearly indicates an NH → O_{water} hydrogen bond and encourages its assignment to structure W1A, for which the predicted shift is 115 cm^{-1}; these values are summarised in Table 2. Figure 7 displays a section of the IR ion dip spectra of 4PI and 4PI(H_2O) recorded in the excited, S_1 state. In the bare molecule, ν(NH) shifts to 3 505 cm^{-1}, 9 cm^{-1} to the red of its frequency in S_0, but in the hydrated complex the NH → O_{water} band (at 3 379 cm^{-1}) shifts 29 cm^{-1} to the red, reflecting the increased acidity at the >NH site following electronic excitation.

4PI$(H_2O)_2$

The UV R2PI spectrum recorded in the 4PI$(H_2O)_2^+$ mass channel was heavily "contaminated" by contributions from higher clusters, principally those with $n = 3$

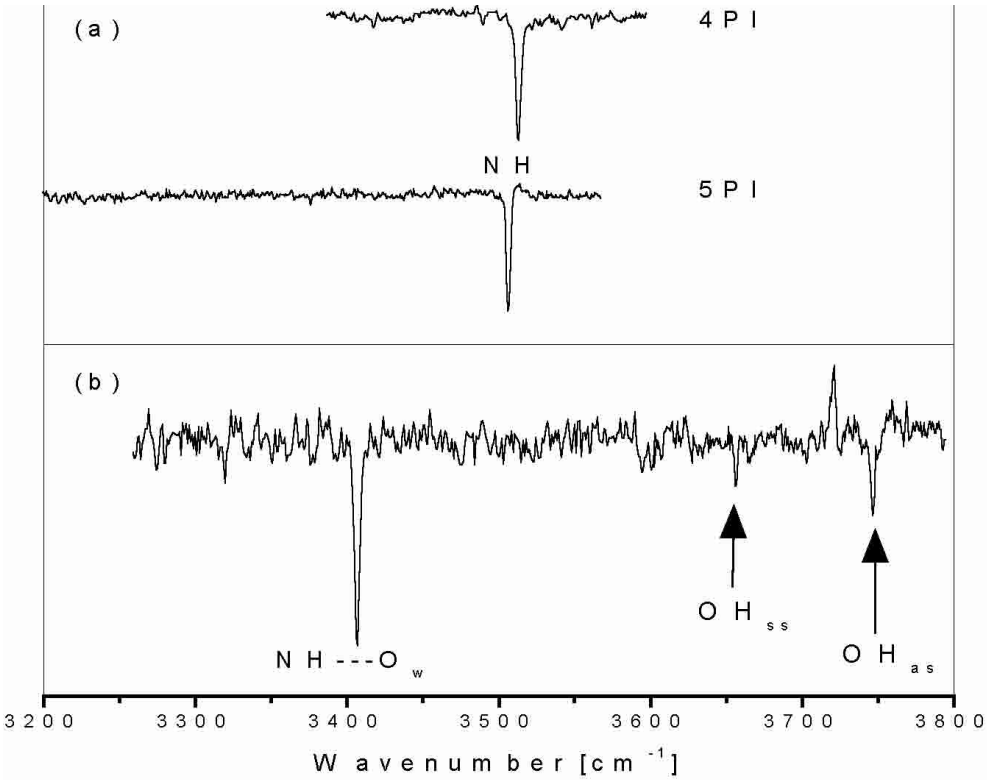

Fig. 6. IR ion dip spectra of (a) 4PI and 5PI and (b) 4PI·(H_2O).

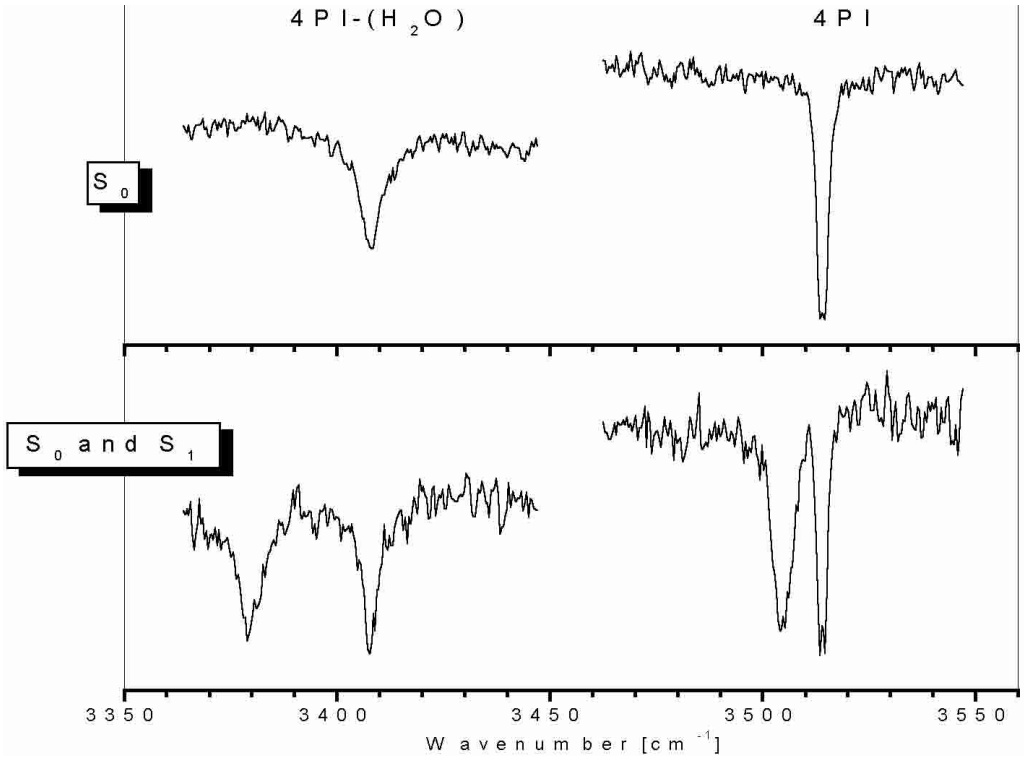

Fig. 7. IR ion dip spectra of 4PI and 4PI·(H_2O) in the S_0 and S_1 states.

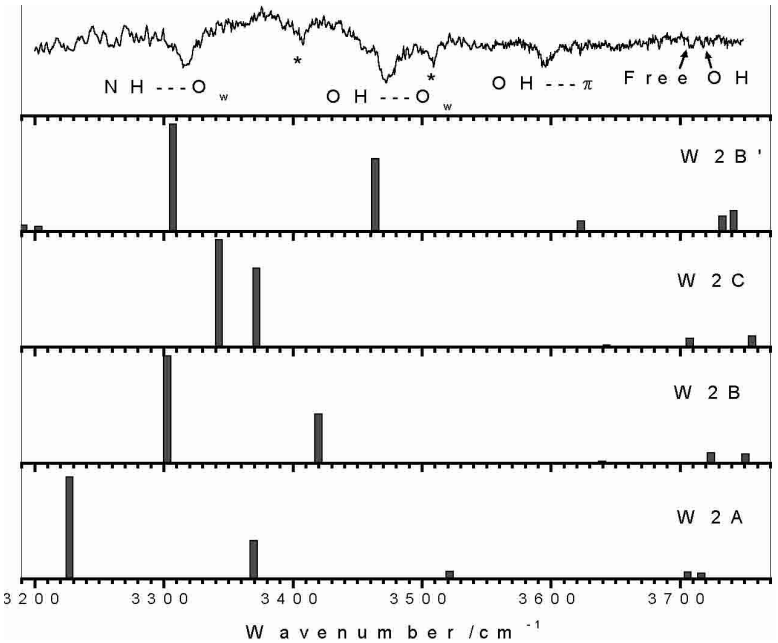

Fig. 8. IR ion dip spectrum and *ab initio* predictions for the 4PI·$(H_2O)_2$ cluster. The two bands marked by an asterisk showed varying relative intensities and are both attributed to different species.

Table 2. Calculated and experimental stretching frequencies of 4PI and 4PI·(H_2O).

	monomer		4PI-(H_2O)		
	Calc.	**Exp.**	W1A	**Exp.**	W1B
NH or NH···O	3 520.1	**3 514**	3 405	**3 407**	3 569
free OH 1			3 762	**3 747**	3 726
free OH 2			3 649	**3 656**	
OH···N					3 435

and 4, but it was possible to identify one band (band D at 34 925 cm^{-1}) that was associated with the doubly hydrated cluster. This was confirmed by its IR ion-dip spectrum (recorded in the 4PI$(H_2O)^+$ mass channel to minimise contamination from higher clusters) shown in Figure 8, together with the predicted frequencies of all four conformers; the predicted and experimental band positions are also listed in Table 3a. Two bands are observed in the region around 3 700 cm^{-1}, at 3 710 and 3 718 cm^{-1} and a third is located at 3 596 cm^{-1}. These band positions are very similar to those observed for the doubly hydrated clusters of indole (In-W2) [31] and *trans*-formanilide (FA-W2) [9], where the water dimer bridges an NH site to the phenyl π-cloud of the molecule. The band at 3 596 cm^{-1} is typical for an OH–π hydrogen bond. The corresponding bands for In-W2 and FA-W2 lie very close, at 3 585 and 3 601 cm^{-1}, respectively.

This clearly identifies the conformer as W2B′, which is the only structure showing a band in this region (at 3 623 cm^{-1}) The two bands at 3 317 and 3 473 cm^{-1} are the NH → O and OH → O H-bonded stretches, respectively. Here again, the OH···O frequency (3 473 cm^{-1}) lies very

Table 3. Calculated and experimental stretching frequencies (cm^{-1}) of (a) 4PI·$(H_2O)_2$, (b) 4PI·$(H_2O)_3$ and (c) 4PI·$(H_2O)_4$. Frequencies are scaled by 0.965 for NH and 0.975 for OH stretches.

(a)

	W2A	W2B	W2B′	W2C	**Exp.**
free OH	3 723	3 757	3 742	3 762	**3 718**
	3 712	3 730	3 733	3 714	**3 710**
		3 646	3 623	3 649	**3 596**
bonded OH, NH	3 522	3 474	3 464	3 395	**3 473**
	3 422	3 303	3 325	3 372	**3 317**
	3 277				

(b)

	W3chain	W3A	W3B	W3C	W3D	**Exp.**
free OH	3 735	3 726	3 734	3 757	3 763	**3 723**
	3 733	3 715	3 730	3 733	3 723	**3 720**
	3 722		3 708	3 713	3 712	**3 713**
				3 647	3 650	
bonded OH, NH	3 425	3 560	3 525	3 469	3 413	**3 451**
	3 414	3 521	3 465	3 384	3 389	**3 422**
	3 373	3 397	3 345	3 311	3 236	**3 402**
	3 339	3 383	3 296			**3 323**
		3 276				

(c)

	W4A	W4B	W4C	W4D	W4E	**Exp.**
free OH	3 730	3 722	3 723	3 761	3 738	**3 721**
	3 728	3 721	3 720	3 727	3 731	**3 718**
	3 721	3 716	3 719	3 704	3 713	**3 714**
	3 711		3 701	3 649	3 706	**3 712**
bonded OH, NH	3 391	3 523	3 419	3 569	3 532	**3 424**
	3 327	3 488	3 338	3 386	3 478	**3 387**
	3 316	3 393	3 338	3 382	3 397	**3 317**
	3 255	3 292	3 268	3 363	3 323	**3 226**
	3 118	3 234		3 266	3 285	

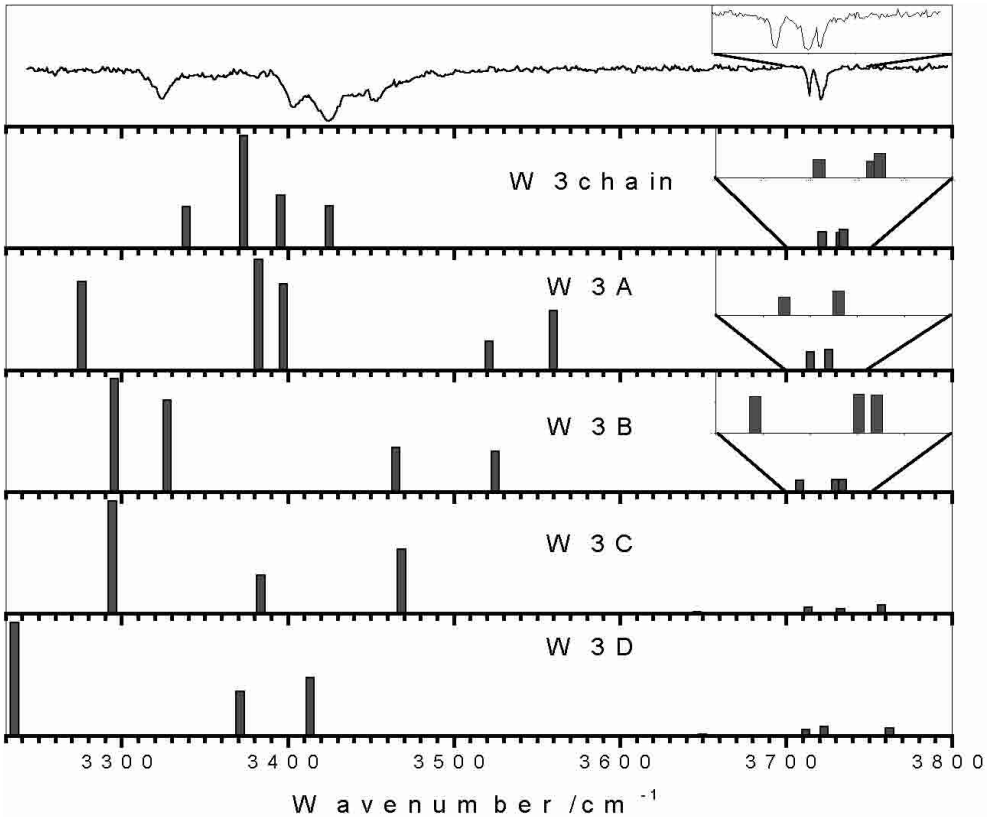

Fig. 9. Experimental and predicted IR spectra for low lying conformers of the 4PI·$(H_2O)_3$ cluster.

close to that observed for In-W2 (3 488 cm^{-1}) and FA-W2 (3 501 cm^{-1}). The NH frequency of the imidazole is now at 3 317 cm^{-1}, further shifted to the red due to cooperativity in the NH → OH → OH → π daisy chain of H-bonds. This shift of 197 cm^{-1} is in line with the calculated shift of 217 cm^{-1} in conformer W2B′. Although the 4PI and indole doubly hydrated clusters are quite similar, the shift of the NH stretching frequency upon double hydration is much higher for 4PI than for indole [32]. This different behaviour of the NH sites of imidazole and indole upon hydration is however not reflected in their gas phase data as the two molecules are reported to have identical deprotonation enthalpies within the experimental errors (1 461±8 kJ mol^{-1} for indole [32] and 1 465±8 kJ mol^{-1} for imidazole [33]). Caution should be exercised when correlating binding energies with spectral shifts.

4PI$(H_2O)_3$

Two bands in the R2PI spectra (labelled A and C in Fig. 5) were associated with the $n = 3$ cluster. Band A is actually a composite band with three components at 34 890, 34 891 and 34 893 cm^{-1}. The central band (34 891 cm^{-1}) appears in the $n = 2$, 3 and 4 mass channels and is associated with the $n = 4$ cluster. The other two, which both generate the same IR spectrum, whether monitored in the $n = 2$ or $n = 3$ cluster ion channel, are associated with an $n = 3$ cluster (the IR spectrum, see Fig. 9, recorded when monitoring the third band at 34 893 cm^{-1}, clearly indicates its association with an $n = 3$ cluster (see below)). The spectra recorded when monitoring band C were identical to those shown in Figure 9 and are not presented.

As shown in Figure 9, the predicted frequencies of the most stable conformer (W3chain) give a very good match with the experimental band positions. A scan at higher resolution in the "free-OH" region clearly identifies three bands, confirming the assignment to the most stable conformer, "W3chain". The four bands located around 3 400 cm^{-1} are associated with the two OH···O modes, and the OH···N and NH···O stretching modes.

4PI$(H_2O)_4$

The UV R2PI spectrum of the $n = 4$ cluster shows a progression of four bands reflecting the excitation of a low frequency mode, with a frequency ∼30 cm^{-1}. This spectrum was obtained following subtraction of the $n = 5$ spectrum from the one recorded in the $n = 4$ channel and is shown as an inset in Figure 5. The first member of the progression, which lies at 34 861 cm^{-1}, is assumed to be the origin; the other members lie at 34 891, 34 922 and 34 951 cm^{-1} respectively, with intensity ratios of 1:1.85:1.36:0.26. The calculated ground state harmonic frequency for the interring torsion is 23.5 cm^{-1}. The structural change in the 4PI$(H_2O)_4$ cluster following electronic excitation, parallels the change identified earlier [23] in the 5PI monomer: 5PI is non-planar in its S_0 ground state but planar in its

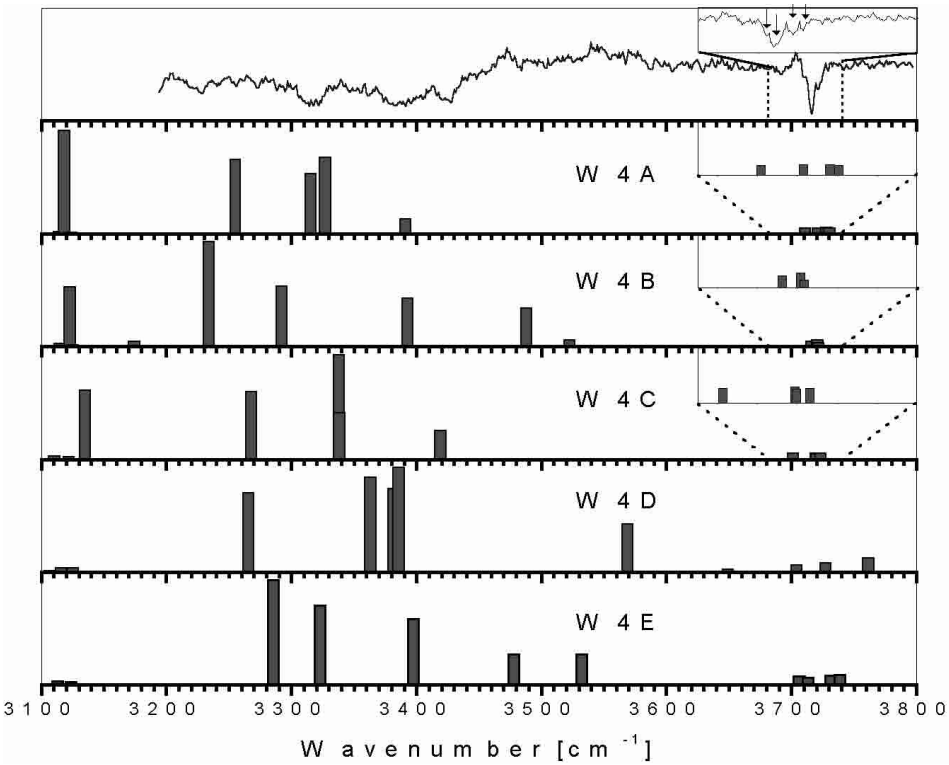

Fig. 10. Experimental and predicted IR spectra for low lying conformers of the 4PI·$(H_2O)_4$ cluster.

excited S_1 state, and its R2PI spectrum [23,24] displays a strong progression in the inter-ring torsional mode. This behaviour is also in agreement with the predicted structure of the most stable conformer of the 4PI$(H_2O)_4$ cluster, W4A, which, unlike the 4PI monomer, has a twisted equilibrium structure with a torsional angle of 18° between the two rings in the ground state. The IR ion-dip spectrum of 4PI$(H_2O)_4$, recorded when monitoring the most intense band of the progression (band A's central component at 34 891 cm^{-1}), is shown in Figure 10; an identical spectrum was also recorded on the band at 34 922 cm^{-1}. Four features appear in the 3 400 cm^{-1} region, at 3 226, 3 317, 3 387 and 3 424 cm^{-1}, in good agreement with the *ab initio* calculations for conformer W4A (see Tab. 3c), which predicts three OH···O and one NH···O vibrational frequencies in that region. The OH···N vibrational mode (although not recorded) is shifted still further to the red, at 3 118 cm^{-1}. Four "free" OH bands appear in the region above 3 700 cm^{-1}; they are very closely spaced but they could be separated by a scan at higher resolution, as shown in the inset in Figure 10. The four bands appear at 3 712, 3 714, 3 718 and 3 721 cm^{-1}.

4 Conclusion

Clusters of 4-phenylimidazole with up to four water molecules have been investigated under supersonic expansion conditions. Their separately resolved IR/UV ion dip spectra, coupled with the results of *ab initio* calculations, have provided sufficient information to allow their individual structural assignment. In each case, the water molecules bind primarily to the NH site of the imidazole ring. The clusters with $n \geq 2$ form linear (as opposed to cyclic) water chains, in which the proton donating terminus bridges either to the π-electron system ($n = 2$) or to the >N: atom site ($n = 3, 4$) on the imidazole ring. Structures in which water molecules are *separately* bound at the >NH and >N: sites to provide a "donor-imidazole-acceptor" unit are not generated; the only way to form such a structure appears to be through a "water wire" bridge benefiting from cooperative effects in the chain of hydrogen bonds. However, the resolved UV and IR spectra of the chain clusters ($n = 2...4$) remain discrete, and provide no evidence of proton transfer either in the excited or in the ground electronic state of the clusters. Even in the most favoured clusters, 4/5PI$(H_2O)_4$, the calculated barrier for proton transfer in the ground state is ∼70 kJ mol^{-1}.

We would like to thank the Leverhulme Trust for their financial support (FOT) and the Physical and Theoretical Chemistry Laboratory for providing laboratory space and support. We are particularly grateful for the fruitful discussions and collaboration with Prof. David W. Pratt in Pittsburgh.

References

1. A . Held, D.W. Pratt, J. Am. Chem. Soc. **115**, 9708 (1993)
2. Y. Matsuda, T. Ebata, N. Mikami, J. Chem. Phys. **110**, 8397 (1999); Y. Matsuda, T. Ebata, N. Mikami, J. Phys. Chem. A **105**, 3475 (2001)

3. G. Florio, C. Gruenloh, R. Quimpo, T. Zwier, J. Chem. Phys. **113**, 11143 (2000)
4. F. Lahmani *et al.*, Chem. Phys. Lett. **220**, 235 (1994)
5. A. Bach, S. Coussan, A. Müller, S. Leutwyler, J. Chem. Phys. **113**, 9032 (2000)
6. J.R. Carney, T.S. Zwier, A.V. Fedorov, J.R. Cable, J. Phys. Chem. A **105**, 3487 (2001)
7. A. Nakajima, M. Hirano, R. Hasumi, K. Kaya, H. Watanabe, C.C. Carter, J.M. Williamson, T.A. Miller, J. Phys. Chem. A **101**, 392 (1997)
8. J. Dickinson, M. Hockridge, E. Robertson, J. Simons, J. Phys. Chem. A **103**, 6938 (1999)
9. E.G. Robertson, Chem. Phys. Lett. **325**, 299 (2000)
10. M. Mitsui, Y. Oshima, S. Ishiuchi, M. Sakai, M. Fujii, J. Phys. Chem. A **104**, 8649 (2000)
11. J. Dickinson, P. Joireman, R. Randall, E. Robertson, J. Simons, J. Phys. Chem. **101**, 513 (1997)
12. J.R. Carney, B.C. Dian, G.M. Florio, T.S. Zwier, J. Am. Chem. Soc. **123**, 5596 (2001)
13. G.F. Velardez, J.C. Ferrero, J.A. Beswick, J.P. Daudey, J. Phys. Chem. A **105**, 8769 (2001)
14. L.C. Snoek, R.T. Kroemer, J.P. Simons, Phys. Chem. Chem. Phys. **4**, 2130 (2002)
15. S. Coussan, M. Meuwly, S. Leutwyler, J. Chem. Phys. **114**, 3524 (2001)
16. M. Meuwly, A. Bach, S. Leutwyler, J. Am. Chem. Soc. **113**, 11446 (2001)
17. T.E. Creighton, *Proteins, Structures and Molecular Properties,* 2nd edn. (W.H. Freeman and Company, New York, 1997), Ch. 9
18. W.W. Bachovchin, Magn. Reson. Chem. **39**, S199 (2001)
19. K. Hasegawa, T. Ono, T. Noguchi, J. Phys. Chem. B **104**, 4253 (2000)
20. D. Lu, G. Voth, J. Am. Chem. Soc. **120**, 4006 (1998)
21. R.R. Sadeghi, H.P. Cheng, J. Chem. Phys. **111**, 2086 (1999)
22. T.S. Zwier, J. Phys. Chem. A **105**, 8827 (2001)
23. M.R. Hockridge, E.G. Robertson, J.P. Simons, Chem. Phys. Lett. **302**, 538 (1999)
24. M.R. Hockridge, E.G. Robertson, J.P. Simons, D.R. Borst, T.M. Korter, D.W. Pratt, Chem. Phys. Lett. **334**, 31 (2001)
25. M.J. Frisch, G.W. Trucks, H.B. Schlegel, G.E. Scuseria, M.A. Robb, J.R. Cheeseman, V.G. Zakrzewski, J.A. Montgomery Jr, R.E. Stratmann, J.C. Burant, S. Dapprich, J.M. Millam, A.D. Daniels, K.N. Kudin, M.C. Strain, O. Farkas, J. Tomasi, V. Barone, M. Cossi, R. Cammi, B. Mennucci, C. Pomelli, C. Adamo, S. Clifford, J. Ochterski, G.A. Petersson, P.Y. Ayala, Q.Cui, K. Morokuma, D.K. Malick, A.D. Rabuck, K. Raghavachari, J.B. Foresman, J. Cioslowski, J.V. Ortiz, B.B. Stefanov, G. Liu, A. Liashenko, P. Piskorz, I. Komaromi, R. Gomperts, R.L. Martin, D.J. Fox, T. Keith, M.A. Al-Laham, C.Y. Peng, A. Nanayakkara, C. Gonzalez, M. Challacombe, P.M.W. Gill, B. Johnson, W. Chen, M.W. Wong, J.L. Andres, C. Gonzalez, M. Head-Gordon, E.S. Replogle, J.A. Pople, *Gaussian*, Inc., Pittsburgh PA, 1998
26. M. Mons, I. Dimicoli, B. Tardivel, F. Piuzzi, E.G. Robertson, J.P. Simons, J. Phys. Chem. **103**, 6938 (1999)
27. L.C. Snoek, E.G. Robertson, R.T. Kroemer, J.P. Simons, Chem. Phys. Lett. **321**, 49 (2000)
28. J.R. Carney, T.S. Zwier, J. Phys. Chem. A **103**, 9943 (1999)
29. S.F. Boys, F. Bernardi, Molec. Phys. **19**, 553 (1970)
30. H. Wolff, E. Wolff, Spectrochim. Acta A **27**, 2109 (1971)
31. J. Carney, F. Hagemeister, T. Zwier, J. Chem. Phys. **108**, 3379 (1998)
32. M. Meot-Ner, J.F. Liebman, S.A. Kafafi, J. Am. Chem. Soc. **110**, 5937 (1998)
33. R.W. Taft, F. Anvia, M. Taagepera, J. Catalan, J. Elgueroy, J. Am. Chem. Soc. **108**, 3237 (1986)